The Meteoritical Society

Meteoritics & Planetary Science 45, Nr 10–11, 1804–1811 (2010)
doi: 10.1111/j.1945-5100.2010.01146.x

The shape and rotation of asteroid 2008 TC_3

Peter SCHEIRICH[1*], Josef ĎURECH[2], Petr PRAVEC[1], Marek KOZUBAL[3], Ron DANTOWITZ[3], Mikko KAASALAINEN[4], Alberto Silva BETZLER[5], Paolo BELTRAME[6], Gustavo MULER[7], Peter BIRTWHISTLE[8], and Francois KUGEL[9]

[1]Astronomical Institute, Academy of Sciences of the Czech Republic, Fričova 1, 25165 Ondřejov, Czech Republic
[2]Astronomical Institute, Faculty of Mathematics and Physics, Charles University in Prague, V Holešovičkách 2, 18000 Prague, Czech Republic
[3]Clay Center Observatory, Dexter and Southfield Schools, 20 Newton Street Brookline, Massachusetts 02445, USA
[4]Department of Mathematics, Tampere University of Technology, P.O. Box 553, FI-33101 Tampere, Finland
[5]Instituto de Física, Universidade Federal da Bahia, Campus Universitário de Ondina, 40210-340, Salvador, Brazil
[6]Circolo Astrofili Talmassons Observatory, Via Cadorna 57, I-33030 Talmassons, Udine, Italy
[7]Nazaret Observatory, Nazaret, 35530, Canary Islands, Spain
[8]Great Shefford Observatory, Phlox Cottage, Wantage Road, Great Shefford, RG17 7DA, UK
[9]Observatoire Chante-Perdrix, Dauban, 04150, France
[*]Corresponding author. E-mail: petr.scheirich@centrum.cz

(Received 21 June 2010; revision accepted 15 October 2010)

Abstract–On October 6, 2008, a small F-class asteroid 2008 TC_3 was discovered by Catalina Sky Survey telescope, and exploded 20 hr later in the Earth's atmosphere at 37 km altitude. We analyzed available photometric data taken from 6 October 21:10 to 7 October 01:46 UT, and created a numerical model of a shape and rotation state of the asteroid. The asteroid was in excited rotational state. We found two approximately mirror solutions of orientation of its angular momentum vector. Rotational and precession periods are 99.20 and 97.00 s (errors of the rotational period for the two solutions are 0.03 and 0.04 s; of the precession period are 0.05 s for both solutions). The volume of the convex model and the length of the longest axis of the dynamically equivalent, equal volume ellipsoid are $p_V^{-3/2} \times 0.25\,m^3$ and $p_V^{-1/2} \times 1.46$ m, where p_V is surface geometric albedo. Assuming a mean albedo value for F taxonomic class, 0.049 ± 0.010, the volume is $(25 \pm 10)\,m^3$ and the longest axis is (6.7 ± 0.8) m. This volume of the convex model is an upper limit on a real volume of the asteroid, which may be less by up to 20% due to concavities.

INTRODUCTION

The asteroid 2008 TC_3 was discovered by the automated Catalina Sky Survey telescope on October 6, 2008, at 06:39 UTC. It impacted the Earth's atmosphere over the Nubian Desert of northern Sudan on 7 October 02:45 UTC (Brown 2008), creating a debris field of Almahata Sitta meteorites (Jenniskens et al. 2009). A reflectance spectrum of the asteroid obtained on October 6 at 22:22–22:28 UTC was classified as F-class in Tholen taxonomy by Jenniskens et al. (2009). They also reported an analysis of 2 hr of photometric data showing apparent frequencies of $1/(49.0338 \pm 0.0007)$ and $1/(96.987 \pm 0.003)\ s^{-1}$ and their linear harmonics, revealing that the asteroid was in a nonprincipal-axis (NPA) rotation state (see also Pravec et al. 2005).

In this article, we analyze available photometric data and derive the rotation state and a shape of the asteroid in more detail. As this is the only case where an asteroid was observed in space prior to its entering the Earth's atmosphere as a bolide leaving meteorites, this information provide an important link between asteroid, meteor, and meteorite sciences. The volume of the asteroid is a key parameter for estimating its density, whereas its orientation is important for modeling of the atmospheric penetration of large meteoroids.

In the Photometric Data and Periods Derivation section, we summarize the available data and present the derivation of periods, a numerical model is described in the Physical Model of Asteroid 2008 TC_3 section. The findings of the modeling are shown in the Results section and the final section concludes.

PHOTOMETRIC DATA AND PERIODS DERIVATION

The photometric data used for the analysis were taken by M. Kozubal and R. Dantowitz (hereafter referred to as K&D) with the 0.64 m telescope at the Clay Center Observatory from 6 October 23:48 to 7 October 01:46, 1719 data points (see Kozubal et al. Forthcoming); by P. Beltrame with the 0.35 m telescope at the Circolo Astrofili Talmassons Observatory from 6 October 21:10 to 21:24, 13 data points; and by G. Muler with the 0.3 m telescope at the Nazaret Observatory from 6 October 22:46 to 23:11, 155 data points (the data taken by P. Beltrame and G. Muler were published in Betzler et al. 2009).

For constraining the numerical model (see below), we also reduced some astrometric data taken by P. Birtwhistle with the 0.4 m telescope at the Great Shefford Observatory from 6 October 19:28 to 19:30, eight data points; and by F. Kugel with the 0.5 m telescope at the Observatoire Chante-Perdrix from 18:46 to 18:51, six data points.

Photometric data of the asteroid 2008 TC_3 were taken also by R. Naves from Montcabrer Observatory (Betzler et al. 2009). We did not use these data in the modeling because of their poor quality, but our result is consistent with them.

All dates and times used in this article are in UTC and have been corrected for light-travel time.

The analysis of the K&D data revealed that two main frequencies and linear combinations of their harmonics are present in the lightcurve. This is interpreted as a NPA rotation. The NPA rotators are also called *tumblers* or *tumbling asteroids* in previous works (Harris 1994; Kaasalainen 2001; Pravec et al. 2005). The standard reduction technique for the photometric data of NPA rotators has been developed and applied in previous works. We refer the reader to Pravec et al. (2005) for detailed description of the methods, and only their most important points are mentioned below.

The NPA rotator lightcurve reduced to unit distances from Earth and Sun and to a given phase angle (we used $G = 0.33$ from Kozubal et al. Forthcoming, for the reduction) can be approximated with a 2-D Fourier series in the following form:

$$F(t) = C_0 + \sum_{j=1}^{m}\left[C_{j0}\cos\frac{2\pi j}{P_\psi}t + S_{j0}\sin\frac{2\pi j}{P_\psi}t\right] + \sum_{k=1}^{m}\sum_{j=-m}^{m}\left[C_{jk}\cos\left(\frac{2\pi j}{P_\psi}+\frac{2\pi k}{P_\phi}\right)t + S_{jk}\sin\left(\frac{2\pi j}{P_\psi}+\frac{2\pi k}{P_\phi}\right)t\right], \quad (1)$$

where C_0 is a mean reduced flux, C_{jk} and S_{jk} are Fourier coefficients of the corresponding linear combination of rotational (P_ψ^{-1}) and precession (P_ϕ^{-1}) frequency. As we cannot tell which of the apparent periods in the lightcurve correspond to precession and rotation based on Fourier analysis only (see the next section), notations P_1 and P_2 are used rather than P_ψ and P_ϕ for the derived periods, and an actual assignment of the apparent periods to rotation and precession is based on subsequent physical modeling.

A signal (amplitude) of the harmonic combination ($jf_1 + kf_2$), where $f_1 = P_1^{-1}$ and $f_2 = P_2^{-1}$, is expressed as:

$$A_{jk}^{\mathrm{norm}} = \frac{\sqrt{C_{jk}^2 + S_{jk}^2}}{C_0}. \quad (2)$$

The Fourier series of the fourth order ($m = 4$) was fitted to the K&D data, the periods estimated were $P_1 = (49.0338 \pm 0.0007)$ and $P_2 = (96.987 \pm 0.003)$ s. The strongest signal is in $2f_2$ ($A^{\mathrm{norm}} = 0.24$); the next two frequencies with strong signal are $2f_1$ ($A^{\mathrm{norm}} = 0.17$) and $2(f_2 - f_1)$ ($A^{\mathrm{norm}} = 0.09$).

PHYSICAL MODEL OF ASTEROID 2008 TC_3

A method of construction of physical models of tumbling asteroids was developed and described by Kaasalainen (2001) and modified by Pravec et al. (2005). We used the technique presented by Pravec et al. (2005) for constraining the periods of the asteroid using ellipsoidal approximation of its shape. Then, a full-parameter optimization including shape derivation was performed using code developed by M. Kaasalainen (2001) and converted to C language by J. Ďurech. The main points of the inversion method are outlined below.

The NPA motion of the asteroid can be described with the following eight parameters:

- I_a and I_b, principal moments of inertia corresponding to axial ratios a/c and b/c of the shape, respectively. The principal moment I_c is normalized to unity. We use the notation where c is always the axis around which the ellipsoid is seen as rotating. There are two modes in which the NPA rotator can exist: the long-axis mode (LAM) where

the asteroid's rotation axis c is the longest one (a/c, $b/c < 1$; I_a, $I_b > 1$), and the short-axis mode (SAM) where the c is the shortest axis (a/c, $b/c > 1$; I_a, $I_b < 1$).

- λ_L and β_L, ecliptic coordinates of a direction of angular momentum vector $\vec{L}$. The angular momentum vector is constant in absence of external forces, and c axis precesses around it.
- ϕ_0 and ψ_0, Euler angles describing the orientation of the ellipsoid at epoch t_0 (see Fig. 1). We use the angles in the so-called x-convention (see Samarasinha and A'Hearn 1991). The Z-axis of the inertial frame is parallel to $\vec{L}$ and the XZ-plane contains a vector directed to vernal equinox. The third Euler angle, θ, is directly related to the other parameters (see Kaasalainen 2001) and therefore it is not used as an independent parameter.
- P_ψ and P_ϕ, the period of rotation around the axis c and the period of precession of the axis c around $\vec{L}$, respectively. The latter is rather an average period of the angle ϕ, because evolution of the angle is not strictly periodic.

The choice of this set of parameters is motivated by a fact that the periods can be estimated from the Fourier analysis of the lightcurve (although ambiguously) and the asteroid's axial ratios can be estimated from lightcurve amplitudes. So, the number of initially unconstrained parameters shrinks to four. Other possible set of parameters and transformations between the sets can be found in Kaasalainen (2001).

A full amplitude of K&D data of 2008 TC_3 corrected to zero phase is 0.69 magnitude (mag) (Kozubal et al. Forthcoming), suggesting approximate ratio of the longest-to-shortest axial ratio of its shape of 1.9. The largest difference between local maxima of the lightcurve was 0.2 mag (after correction to zero phase), suggesting the longest-to-intermediate axial ratio of 1.2. These values were used as initial estimates for subsequent modeling.

As pointed out by Kaasalainen (2001), main peaks in the Fourier spectrum of a lightcurve of the NPA rotator usually have frequencies equal to $2f_\phi$, $2(f_\phi \pm f_\psi)$, f_ϕ. Given the two observed frequencies in K&D data of 2008 f_1 and f_2, there are eight physically possible combinations for f_ϕ and f_ψ resulting from pairs of equations $f_1 = 2f_\phi$ and $f_2 = 2(f_\phi + f_\psi)$; $f_1 = 2f_\phi$ and $f_2 = 2(f_\phi - f_\psi)$, etc.

We tested all these combinations using the ellipsoidal approximation of the shape with the dimension ratios estimated above as initial values of its axes; the LAM and the SAM modes were tested for each of these combinations. Starting from an equidistant grid of the angles (λ_L, β_L, ϕ_0, and ψ_0), all the eight parameters were iterated to reach the best fit

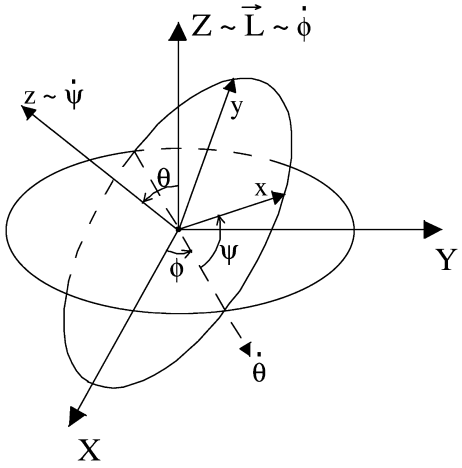

Fig. 1. Inertial reference frame XYZ, the body-frame coordinate system xyz and Euler angles ϕ, ψ, θ describing the orientation of the body.

with the data of K&D, P. Beltrame, and G. Muler (see Pravec et al. 2005, for details of the optimization process). We found only one consistent combination of the frequencies: $f_1 = 2(f_\phi + f_\psi)$ and $f_2 = 2f_\phi$, giving periods $P_\psi = 99.17$ and $P_\phi = 96.99$ s, and the rotation being in the LAM mode.

Using these two periods and best-fit values of ϕ_0, ψ_0, I_a, and I_b, we constructed an equidistant grid of (λ_L, β_L). For each point of this grid, angles ϕ_0 and ψ_0 were recomputed for each combination of λ_L and β_L so that an orientation of the fitted ellipsoid at a few rotational phases mimics the observed lightcurve. Using the parameters from this grid as initial guesses, optimization of convex shape and ϕ_0, ψ_0, I_a, I_b, P_ψ, and P_ϕ was performed. Angles λ_L and β_L were fixed during the optimization—this allows us to constrain their uncertainty region (see below).

Photometric behavior of the surface was described by Hapke's photometric function for a rough surface (Bowell et al. 1989) with parameters $w = 0.24$, $g = -0.49$, $h = 0.11$, $S_0 = -0.3$, $\bar{\theta} = 20°$. We found that the model is only weakly sensitive to these parameters; the set presented here is only one of several others giving satisfactory fit.

The two principal moments I_a and I_b were fitted as independent dynamical parameters. As actual moments of inertia of the fitted shapes differ slightly from I_a and I_b, the shapes were stretched so that their moments of inertia match the fitted values I_a and I_b as much as possible. We compared synthetic lightcurves generated using the shapes before and after the stretching and found only insignificant differences. The moments of inertia shown in Table 1 are computed from the stretched shapes; the moments fitted as dynamical parameters are within their error bars.

Table 1. Parameters of the two best-fit solutions with their estimated 3σ errors.

Parameter	Solution I	Solution II
Fitted parameters		
RMS (magnitude)	0.079	0.083
λ_L (°)	90^{+9}_{-50}	275^{+5}_{-14}
β_L (°)	-36^{+20}_{-50}	$+3^{+40}_{-25}$
ϕ_0 (°)	327 ± 20	356^{+15}_{-27}
ψ_0 (°)	345 ± 1	165^{+4}_{-2}
P_ψ (s)	99.19 ± 0.03	99.20 ± 0.04
P_ϕ (s)	96.99 ± 0.05	97.02 ± 0.05
I_a	$3.196^{+0.004}_{-0.009}$	$3.202^{+0.005}_{-0.01}$
I_b	$2.798^{+0.005}_{-0.01}$	$2.798^{+0.01}_{-0.007}$
Derived parameters		
a_{dyn}/c_{dyn}	$0.3469^{+0.0003}_{-0.0006}$	$0.3451^{+0.0042}_{-0.0001}$
b_{dyn}/c_{dyn}	$0.5293^{+0.0014}_{-0.0007}$	$0.5300^{+0.0007}_{-0.0036}$
a/c	$0.36^{+0.01}_{-0.03}$	$0.35^{+0.05}_{-0.02}$
b/c	$0.55^{+0.01}_{-0.07}$	$0.54^{+0.02}_{-0.04}$
$\delta_{(x,radiant)}$ (°)	56^{+15}_{-23}	28 ± 15
$\delta_{(z,radiant)}$ (°)	86^{+17}_{-24}	114^{+17}_{-29}

Note: See text for explanation of the symbols.

For each best-fit set of shape and parameters, synthetic lightcurves were constructed and visually compared with the observed data used to fitting, as well as with the data taken by P. Birtwhistle and F. Kugel. The solutions whose lightcurves did not match these data were excluded. The comparison was made on an experience that 3σ error is usually clearly distinguishable when comparing the lightcurves. Parameters respective to the plausible selected curves therefore represent 3σ ranges of the solutions.

RESULTS

Two best-fit, approximately mirror, solutions were found. The best-fit values of modeled parameters and their 3σ errors are summarized in Table 1. We report two kinds of axial ratios of the shape there. a_{dyn}/c_{dyn} and b_{dyn}/c_{dyn} are axial ratios of dynamically equivalent ellipsoid, i.e., an ellipsoid with the same values of principal moments of inertia, defined as:

$$\left(\frac{a_{dyn}}{c_{dyn}}\right)^2 = \frac{I_b - I_a + 1}{I_a + I_b - 1}, \quad \left(\frac{b_{dyn}}{c_{dyn}}\right)^2 = \frac{I_a - I_b + 1}{I_a + I_b - 1}. \quad (3)$$

a/c and b/c are dimension ratios of the convex shape model along its principal axes. The regions of plausible values of λ_L and β_L are plotted in Fig. 2 together with their best-fit values. The convex shape models of these two solutions are presented in Fig. 3. The synthetic lightcurves of the best-fit solutions together with samples of K&D data in five epochs are presented in Fig. 4.

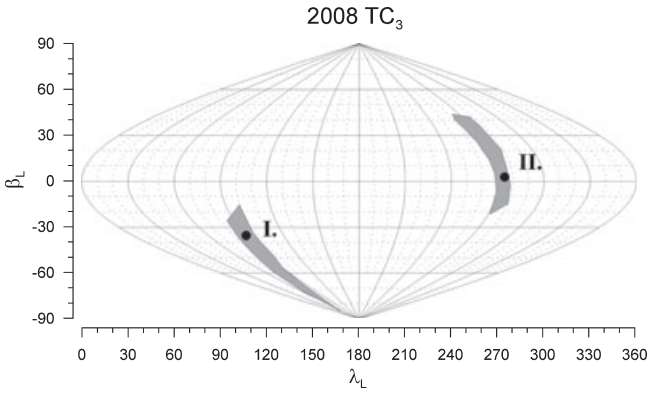

Fig. 2. Range of plausible directions of the angular momentum vector in ecliptic coordinates (gray areas). The best-fit solutions are marked by filled circles.

Absolute dimensions of the asteroid can be scaled using its absolute magnitude H and surface geometric albedo p_V by a formula (see Pravec and Harris 2007):

$$D\sqrt{p_V} = K \times 10^{-H/5}, \quad (4)$$

where K = 1329 km and D is an effective diameter of the object. D was determined from the shape model and rotation parameters by time-averaging over interval of K&D data as $\pi D^2/4 = (0.27 \pm 0.02)\cdot c^2$ (the value is the same for both solutions). The absolute magnitude was determined by Kozubal et al. (Forthcoming) as $H = 30.86 \pm 0.01$. The surface geometric albedo of the asteroid is unknown. Albedo measurements of the meteorite samples range from 0.1 to 0.23 (Hiroi et al. 2010), but these are albedos of fresh surfaces unaffected by space weathering, which is expected to lower surface albedo up to 50% (Clark et al. 2002). We calculated the absolute size of the convex model for albedos in range from 0.04 to 0.25. The results in the form of volume and length of the longest axis c are shown at top panel of Fig. 5. For p_V = 0.10, the volume is (7.8 ± 0.4) m^3 and c = (4.6 ± 0.2) m (3σ errors; the values are the same for the both solutions). The volume and c scale as $p_V^{-3/2}$ and $p_V^{-1/2}$, respectively. A slope parameter G (Bowell et al. 1989) corresponding to the H-value is $G = 0.33 \pm 0.03$ (Kozubal et al. Forthcoming). This value is out of range of values measured for asteroids with albedos of approximately 0.04–0.2 (Warner et al. 2009). We refer the reader to Kozubal et al. (Forthcoming) for discussion of this discrepancy.

Note that the volume of the convex model is an upper limit of a volume of real figure of the asteroid due to concavities which are likely present. We

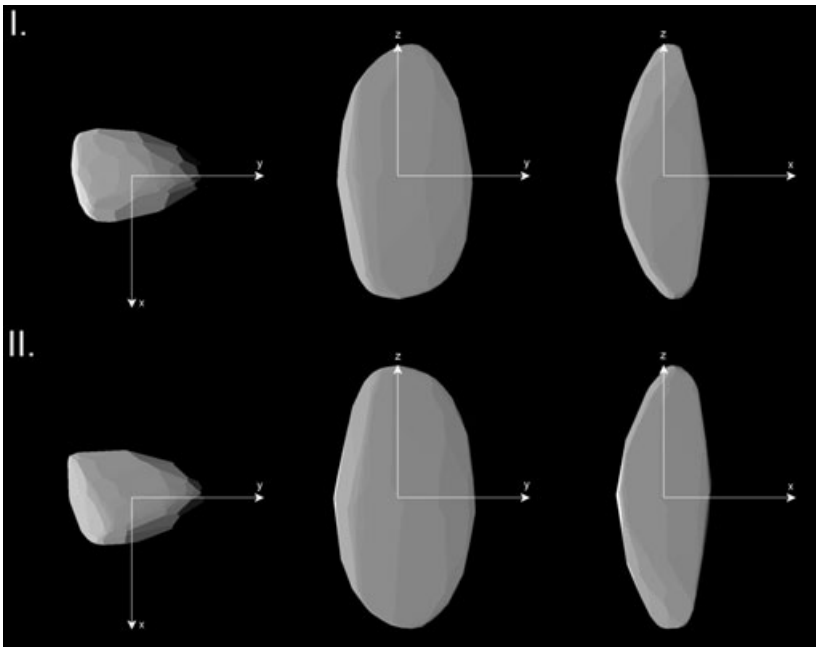

Fig. 3. The two shape models of 2008 TC_3 from the best-fit solutions I (top) and II (bottom). Both models are shown in three viewing geometries; x and z are axes with the greatest and the lowest moments of inertia, respectively.

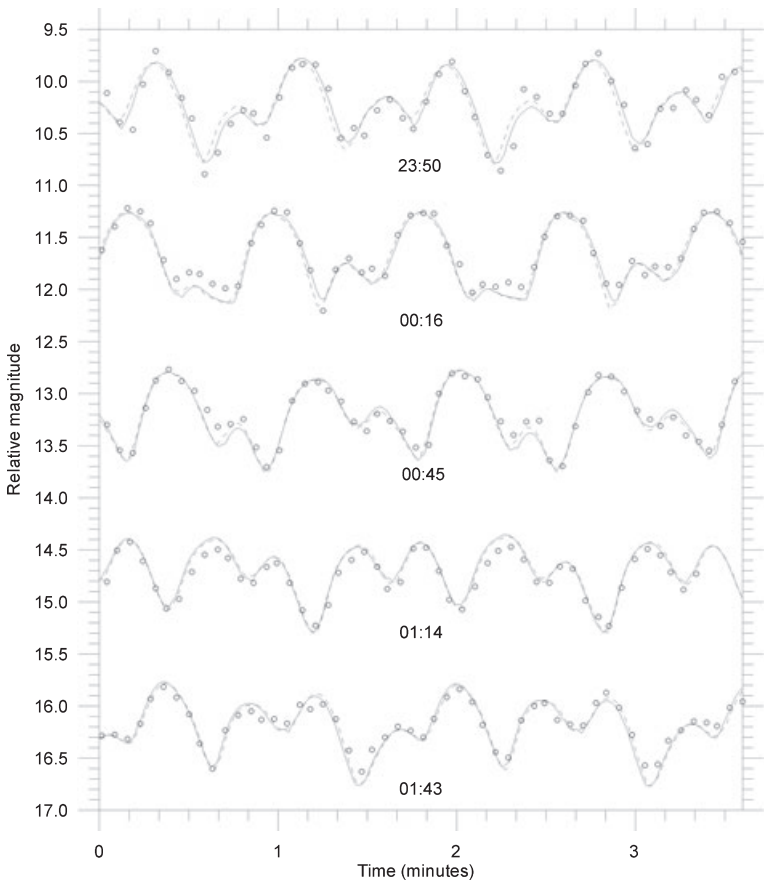

Fig. 4. Lightcurve data (open circles) of K&D shown for five different epochs. Curves are the best-fit synthetic lightcurves for the solution I (solid line) and II (dashed line). Midtimes of the sequences from 6 October 23:50 to 7 October 01:43 (UT) are shown below each lightcurve. The sequences are vertically offset by 1.5 mag for clarity.

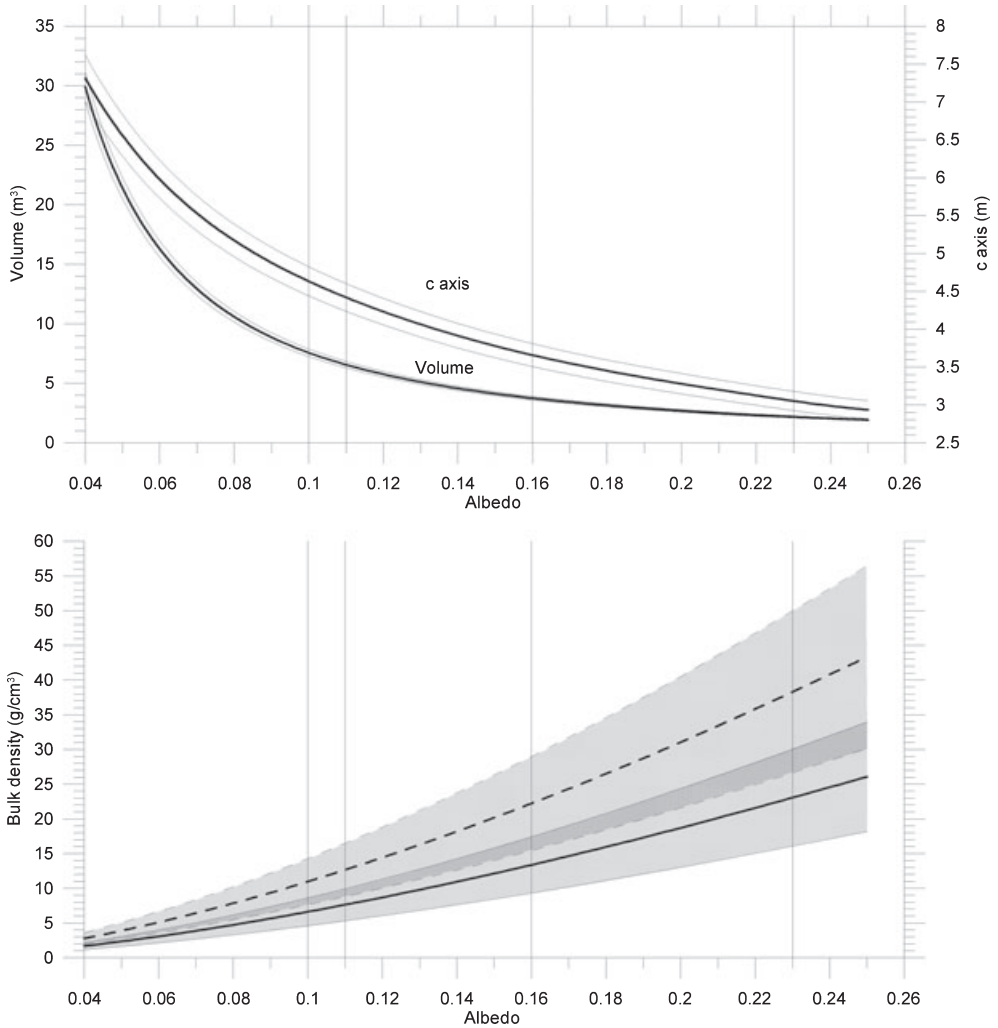

Fig. 5. Top: volume and the largest axis of the shape model, with 3σ errors indicated, as a function of surface geometric albedo. Bottom: Bulk densities of the asteroid derived from estimates of its mass taken from Borovička and Charvát (2009) (solid line) and from Jenniskens et al. (2009) (dashed line), with 3σ errors indicated, as a function of surface geometric albedo. The vertical lines are geometric albedos measured for Almahata Sitta meteorite fragments by Hiroi et al. (2010).

compared volumes of convex models of (433) Eros and (25143) Itokawa derived from photometry (Kaasalainen et al. 2001, 2003) with volumes of their real figures (Gaskell 2008; Gaskell et al. 2008); the differences are 12% for Eros and 5% for Itokawa. Therefore, we use a conservative estimate of the difference between the volume of the convex model and the real figure of 20%.

We address the mass estimates reported previously. Jenniskens et al. (2009) and Borovička and Charvát (2009) reported masses of (83 ± 25) and (50 ± 15) t, respectively. We calculated the bulk densities of the asteroid from these mass estimates and the volumes for albedos in range from 0.04 to 0.25; the results are shown at bottom panel of Fig. 5. For mass of (83 ± 25) t, the values of the bulk density are unrealistically high for albedo of 0.07 or higher (the density is 6 ± 2 g cm^{-3} for albedo = 0.07). For mass of (50 ± 15) t, the values of bulk density are unrealistically high for albedo of 0.09 or higher (the density is 5.5 ± 1.7 g cm^{-3} for albedo = 0.09). The bulk densities of the Almahata Sitta meteorites are in range 2.8–3.7 g cm^{-3} (Kohout et al. unpublished data) and the bulk density of the asteroid is expected to be even lower due to macroporosity. If the geometric albedo of the surface of asteroid was close to the albedo of the meteorite fragments, than we would suggest that the mass from Borovička and Charvát (2009) is slightly overestimated, and the mass from Jenniskens et al. (2009) is highly overestimated. The issue of the macroporosity and the bulk density of the asteroid 2008 TC_3 is further investigated by Kohout et al. (unpublished data).

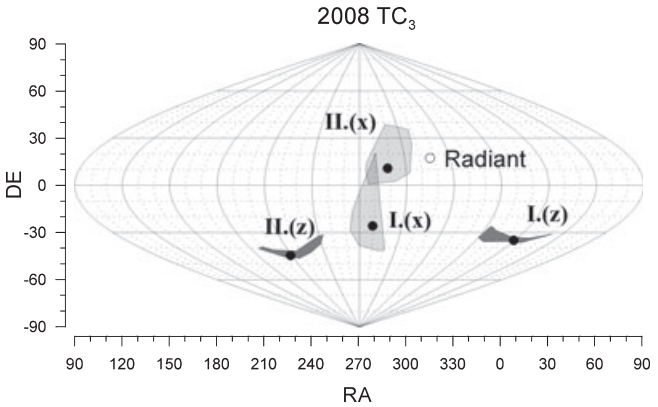

Fig. 6. Range of plausible directions of the shortest (x) and the longest (z) axis at the moment of the asteroid being at 100 km height (shaded areas) in equatorial coordinates. The best-fit solutions are marked by filled circles. The direction of the asteroid's vector of motion (radiant) is marked by open circle.

Lastly, we briefly address an orientation of the asteroid 2008 TC_3 at a moment of its atmospheric entry, as it may be important information for future modeling of the atmospheric penetration. The asteroid reached a height of 100 km above the surface of Earth at Julian date 2454746.614936227. The bolide radiant (i.e., a vector opposite to the motion) was at right ascension 316.8° and declination +17.2° (Chesley, personal communication). We calculated orientations of the asteroid's longest and shortest axes at this time for 3σ regions of the both solutions and compared them with the radiant. The results are shown at Fig. 6. Angles between the axes and the radiant for the best-fit solutions and their errors are presented in Table 1 as $\delta_{(x,\text{radiant})}$ (the shortest axis) and $\delta_{(z,\text{radiant})}$ (the longest axis). A cross section of the convex model along the direction of the radiant at the height of 100 km is $(0.27 \pm 0.04)\cdot c^2$ (3σ error; the values are the same within the error bars for the both solutions).

CONCLUSIONS

The asteroid 2008 TC_3 was precessing body in LAM mode with period of rotation of 99.2 s and period of precession of 97.0 s. We found two approximately mirror solutions of orientation of its angular momentum vector and obtained its shape using convex modeling of photometric data. The shape has axial ratio of approximately 1:0.54:0.36. The volume of the convex model and the length of the longest axis of the dynamically equivalent, equal volume ellipsoid for both solutions are $p_V^{-3/2} \times 0.24\ \text{m}^3$ and $p_V^{-1/2} \times 1.46$ m, respectively, where p_V is the surface geometric albedo. The actual albedo of the asteroid is unknown, but using a mean albedo value in V filter for F taxonomic class, 0.049 ± 0.010 (Warner et al. 2009), gives the upper limit of volume of the real figure of (25 ± 10) m^3 and the longest axis of (6.8 ± 0.8) m. This is in good agreement with mass estimates reported by Jenniskens et al. (2009): (83 ± 25) t, giving a lower limit of bulk density of (3.3 ± 1.7) g cm^{-3}, and by Borovička and Charvát (2009): (50 ± 15) t, giving a lower limit of bulk density of (2.0 ± 1.0) g cm^{-3} (bulk densities of Almahata Sitta meteorites, reported by Kohout et al. unpublished data, are in range 2.8–3.7 g cm^{-3}), the error bars are 1σ. If, however, the surface albedo is close to the albedos of the meteorites reported by Hiroi et al. (2010), which are in the range 0.1–0.23, then the masses are overestimated.

The orientation of the asteroid at the moment it entered the atmosphere, assuming this was at a height of 100 km, was such that its longest axis formed an angle with its vector of motion of $(86^{+17}_{-24})°$ or $(114^{+17}_{-29})°$ for the solutions I and II, respectively.

The observed data, convex shape model, and the rotational state of the asteroid 2008 TC_3 will be accessible in DAMIT database (Ďurech et al. 2010) at http://astro.troja.mff.cuni.cz/projects/asteroids3D.

Acknowledgments—The work at Charles University (J. Ďurech) was supported by the Grant Agency of the Czech Republic, Grant P209/10/0537, and by Ministry of Education, Youth, and Sports of the Czech Republic, Grant MSM0021620860. We thank Alan Harris for his valuable review of the article.

Editorial Handling—Dr. Dina Prialnik

REFERENCES

Betzler A. S., Beltrame P., Naves R., and Muler G. 2009. Photometric observations of Earth-impacting 2008 TC_3. *Minor Planet Bulletin* 36:58–59.

Borovička J. and Charvát Z. 2009. Meteosat observation of the atmospheric entry of 2008 TC_3 over Sudan and the associated dust cloud. *Astronomy & Astrophysics* 507:1015–1022.

Bowell E., Hapke B., Domingue D., Lumme K., Peltoniemi J., and Harris A. W. 1989. Application of photometric models to asteroids. In *Asteroids II*, edited by Binzel R., Gehrels T., and Matthews M. S. Tucson, Arizona: The University of Arizona Press. pp. 524–556.

Brown P. G. 2008. *US Government release: Bolide detection notification 2008-282*. http://aquarid.physics.uwo.ca/~pbrown/usaf/usg282.txt. Accessed October 15, 2008.

Clark B. E., Hapke B., Pieters C., and Britt D. 2002. Asteroid space weathering and regolith evolution. In *Asteroids III*, edited by Bottke W. F. Jr., Cellino A., Paolicchi P., and Binzel R. P. Tucson, Arizona: The University of Arizona Press. pp. 585–599.

Ďurech J., Sidorin V., and Kaasalainen M. 2010. DAMIT: A database of asteroid models. *Astronomy & Astrophysics* 513:A46.

Gaskell R. W. 2008. *Gaskell Eros Shape Model V1.0. NEAR-A-MSI-5-EROSSHAPE-V1.0*. NASA Planetary Data System.

Gaskell R., Saito J., Ishiguro M., Kubota T., Hashimoto T., Hirata N., Abe S., Barnouin-Jha O., and Scheeres D., 2008. *Gaskell Itokawa Shape Model V1.0. HAY-A-AMICA-5-ITOKAWASHAPE-V1.0*. NASA Planetary Data System.

Harris A. W. 1994. Tumbling asteroids. *Icarus* 107:209–211.

Hiroi T., Jenniskens P., Bishop J. L., Shatir T. S. M., Kudoda A., Shaddad M. H. 2010. Bidirectional visible-NIR and biconical FT-IR reflectance spectra of Almahata Sitta meteorite samples. *Meteoritics & Planetary Science* 45. This issue.

Jenniskens P., Shaddad M. H., Numan D., Elsir S., Kudoda A. M., Zolensky M. E., Le L., Robinson G. A., Friedrich J. M., Rumble D., Steele A., Chesley S. R., Fitzsimmons A., Duddy S., Hsieh H. H., Ramsay G., Brown P. G., Edwards W. N., Tagliaferri E., Boslough M. B., Spalding R. E., Dantowitz R., Kozubal M., Pravec P., Borovička J., Charvat Z., Vaubaillon J., Kuiper J., Albers J., Bishop J. L., Mancinelli R. L., Sandford S. A., Milam S. N., Nuevo M., and Worden S. P. 2009. The impact and recovery of asteroid 2008 TC_3. *Nature* 458:485–488.

Kaasalainen M. 2001. Interpretation of lightcurves of precessing asteroids. *Astronomy & Astrophysics* 376:302–309.

Kaasalainen M., Torppa J., and Muinonen K. 2001. Optimization methods for asteroid lightcurve inversion II. The complete inverse problem. *Icarus* 153:37–51.

Kaasalainen M., Kwiatkowski T., Abe M., Piironen J., Nakamura T., Ohba Y., Dermawan B., Farnham T., Colas F., Lowry S., Weissman P., Whiteley R. J., Tholen D. J., Larson S. M., Yoshikawa M., Toth I., and Velichko F. P. 2003. CCD photometry and model of MUSES-C target (25143) 1998 SF36. *Astronomy & Astrophysics* 405:L29–L32.

Kozubal M. J., Gasida F. W., Dantowitz R. F., Scheirich P., and Harris A. W. Forthcoming. Photometric observations of earth-impacting asteroid 2008 TC_3. *Meteoritics & Planetary Science*.

Pravec P. and Harris A. W. 2007. Binary asteroid population 1. Angular momentum content. *Icarus* 190:250–259.

Pravec P., Harris A. W., Scheirich P., Kušnirák P., Šarounová L., Hergenrother C. W., Mottola S., Hicks M. D., Masi G., Krugly Yu. N., Shevchenko V. G., Nolan M. C., Howell E. S., Kaasalainen M., Galád A., Brown P., Degraff D. R., Lambert J. V., Cooney W. R., and Foglia S. 2005. Tumbling asteroids. *Icarus* 173:108–131.

Samarasinha N. H. and A'Hearn M. F. 1991. Observational and dynamical constraints on the rotation of comet P/Halley. *Icarus* 93:194–225.

Warner B. D., Harris A. W., and Pravec P. 2009. The asteroid lightcurve database. *Icarus* 202:134–146.